

A Deep-Learning Model Based on Transfer-Learning Technique for Detecting and Classifying Anomalies in Lungs Images

Bassant Mostafa
Computer science department
Higher Technological Institute
Tenth of Ramadan, Egypt

Mohamed Sakr
Computer Science department
Faculty of Computers and Information
Menoufia University
Menoufia, Egypt

Arabi Keshk
Computer Science department
Faculty of Computers and Information
Menoufia university
Menoufia, Egypt

Abstract— Over the past decade, there has been a marked increase in interest in the automated identification of malignant tumors, largely due to the demand for an early and precise diagnosis that would lead to the best available therapy for the impending risk. As part of this effort, a variety of machine-learning and artificially intelligent approaches have been used to produce reliable aiding tools. To improve the automatic recognition and diagnosis of problematic lung areas, a deep learning model relying on the transfer learning approach is constructed in this research. VGG16, VGG19, and Inception-V3 are employed for the extraction of features from the IQ-OTHNCCD lung cancer dataset. According to experimental findings, transfer-learning models employing the SVM classifier were more effective than those utilizing the softmax function classifier at classifying CT scan images of the used dataset. Results from experiments demonstrate that the VGG19 model is effective for diagnosing lung cancer exceeding other existing models utilizing the same dataset.

Keywords— Machine learning, transfer learning, deep learning, lung cancer, biomedical image classification.

I. INTRODUCTION

When describing anomalies in medical imaging, it's usual to use this term to describe an uncommon variance from the usual. As a result, the phrase “anomaly detection” is encouraged to be used in the field of medicine [1], This satisfies the requirements for outliers (or anomalies) in the data[2]. According to the WHO, 2.21 million cases were reported in 2020, but 1.80 million people died from lung cancer (LC) [3], LC maturation can impair breathing and distribute to several bodily regions, The two primary contributors to risk for the onset of LC are nicotine use and alcoholism, They are responsible for over 80% of LC deaths, and a lot more have been brought on by passive smoking. That explains the fact of While many LC patients have smoked in the past, many others have never smoked [4]. Radon, secondhand smoke, environmental pollution, and other factors can cause LC for nonsmokers [5], Furthermore, cancer may also affect the lungs if it already exists in another section of the body. Early discovery, therefore, offers a decent chance of survival and can help in lowering cancer's aggressiveness, as compared

to cancer remediation found in the initial phases, the likelihood of remaining alive in the more severe form is lower [2], particularly if diagnosed at a very advanced stage, LC is linked to large rates of fatal complications and illness[6], Approximately 80% of cancer cases are accurately identified in the intermediate or terminal instances of the illness [7][8]. To identify lung tumors early, a variety of imaging methods are utilized, such as “computerized-tomography” (CT), X-rays, and “magnetic- resonance-imagery” (MRI), Tumors are categorized into two categories for detection: (i) non-cancerous (benign) tumors; and (ii) cancer-causing (malignant) tumors [3]. The prognosis of cancer of the lungs usually depends on the skill of the treating doctor, However, there's a prospect for "False-positives" which could be damaging to the patient's psychological and financial well-being. Considering this, the application of image processing techniques can improve manual analysis and may benefit radiologists in instantly spotting lung lesions at their earliest phase. For optimal effectiveness and accuracy, Many AI-driven CAD methods for diagnostic use have been developed [3][4]. CT images have some major competitive advantages over other imaging modalities, including quick collection times, cost-effectiveness, and accessibility [9], As a result, CAD systems employ CT images as a starting point for their analysis of LC [6]. The two primary parts of many CAD systems are i) concentrating on dividing lung lesions into segments, and ii) categorizing worrisome lung lesions. Assuming that the first subsystem is handled flawlessly, we consider the second one [10], where A deep learning-powered CAD framework is anticipated to show tremendous potential for the precise automatic lung lesions identifying in clinical visualization and to resolve the problems brought on by delayed and inaccurate diagnosis [11][12][13]. To identify LC using CT images, this study investigates the application of TL which refers to a method whereby the knowledge acquired by a learning approach using data from merely one resource is transferred to address a different but connected issue using newly gathered data, despite the fact that the new task's data availability is limited [14]. Additionally, the performance of DL models may be impacted by issues with visualization of features, construction, model parameter selection, and bias and weights

settings.[15][16]. Consequently, in order to address these concerns and develop an accurate prediction model, the process of identifying LC from CT lung scans is accomplished using the expertise obtained via training of varying CNN on a significant, huge dataset that is called ImageNet. Enhancing classification accuracy and accelerating learning are TL's two main benefits. Following pre-training with the help of initial data, the network parameters are subsequently used in the target domain, and lastly, they are adjusted for enhanced performance [7]. Regarding this, an architecture for LC identification and categorization relying on TL is provided. The model suggested primarily incorporates two parts: i) Noise reduction, equalization of the histogram, segmentation, analyzing morphology, images scaling, splitting of data, and data augmenting are the preliminary component's six primary methods for improving the images of the lungs. ii) Secondly, A fine-tuned pre-trained CNN, such as the InceptionV3, VGG16, or VGG19, is used to categorize LC using the newly learned parameters. The ultimate objectives of this paper are the automatic segmentation of the afflicted region, minimizing the training time, and the enhancement of classification performance. This study attempts to provide main contributions as follows according to the performed survey about the related area in which we are interested:

- 1) We have designed a model that uses the TL process to categorize the patients' LC severity, the system predicts the type using CT images as its input, assisting in the earliest possible contour intervention, and this model is the first of its kind to be used with this dataset.
- 2) Decreasing the training time by removing the unaffected areas from lung images.
- 3) Using morphological analysis, histogram equalization, and noise reduction techniques to enhance affected areas detection.
- 3) Modifying the classifier in the pre-trained networks to improve classification performance.

II. RELATED WORK

Recent years have shown the potential utility of machine-learning models depending on biological data for the diagnosis and prognosis of cancer patients[17], also several studies are being conducted using DL methods[18]. Early cancer cell diagnosis is necessary, no matter what organ it affects. A novel residual neural-network was created by Wang et al. [19] that determines the pathological class of LC and is used to analyze CT image data. Using transfer learning and a public dataset, the model that was suggested is constructed. The test's findings revealed an accuracy rate of 85.71 percent. Additionally, Zheng et al.[20] advocated making use of (R2MNet) to assess the malignancy of lung lesions in the (LIDC-IDRI) dataset. Their findings demonstrate that the suggested methodology has AUCs for nodule radiology-analysis and nodule malignancy-evaluation of 96.27% and 97.52%, respectively. Residual-learning was used by Bhatia et al. [21] to offer a technique for LC detection with CT data. To prepare the data for more in-depth analysis, feature extraction and preprocessing were performed on it. They used the XGBoost and Random-forest techniques following the use of the

ensemble methodology built upon the individual classifiers. They outperformed past studies, achieving 84% on the (LIDC-IDRI) dataset. Chen et. Al. [22] discussed the use of ROI extraction as a method for LC segmenting that concentrates on pulmonary lesions. Combination loss and data augmentation were also employed to enhance the outcomes of training. Despite the infection's area having fuzzy boundaries and morphological modifications, The 3-D Attention Modules can still concentrate on boundary-contouring data. This allows the network to find out more about the spot of interest. Kim. Et.al.[23] They developed an algorithm for precisely diagnosing asbestos-related diseases by combining deep learning methods and the lung segmenting approach. The Threshold-based segmenting procedure may quickly retrieve visualizations of the lungs from a huge CT image file. It functions better when combined with the deep learning technique than when using the original image. Lu. Et.al. [24] employed a (CNN) designed specifically to find LC. The results of the suggested method are compared using ResNet-18, Google-LeNet, AlexNet, and VGG-19. The suggested approach was trained using both the conventional method and an innovative metaheuristic-based method (MPA). Nasser et. al. [25]proposed an ANN-based LC detection model with a 96.67% accuracy percentage. Using AlexNet CNN as a foundation, Agarwal et al. [26] suggested a system for classifying and recognizing LC. They used multilevel thresholding to distinct the lung areas. Using morphology and thresholding-based segmenting methods, the impacted and unaffected regions were separated. AlexNet-CNN was able to differentiate cancerous from tumors that are not cancerous with 96% accuracy after segmenting the tumor locations. ResNet50, Le-Net, VGG16, AlexNet, and InceptionV1 have each been analyzed and evaluated against one another. for the identification of LC using publically available LUNA16 datasets, according to a study proposed by Mosavi et al. [27] Numerous performance optimizers were used for this retrospective study, including SGD, RMSProp, and Adam. Finally, A system for finding nodules in lung tissue incorporating statistical and shape-based characteristics in scans from CT was presented by Khehrah et al.[28]. Table. 1. offers an overview of previous related research. The limitations of earlier research are mentioned.

III. MATERIALS AND PROCEDURES

A. Overall view of the framework

The envisioned system steps go through collecting data, preprocessing, segmenting, feature extraction, and classifying. As demonstrated in Fig.1, after acquiring the images and putting them through the preprocessing stages, the type of abnormality diagnosis was made using the TL model, and after the classification is done the model evaluation is performed using performance measurements.

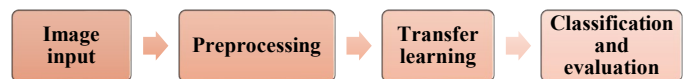


Figure 1. The basic steps of the indicated model

Table 1. Summary of the literature survey on LC detection methods.

Author	dataset	methods	Limitations	results
Wang et al. [19]	Luna 16	newly developed residual NN	Inconsistent data	85.71%
Zheng et al. [20]	LIDC-IDRI	(R2Mnet)	Improved accuracy needed	Accuracy: 89.90% AUC: 96.27%
Bhatia et al. [21]	LIDC-IDRI	ResNet XGBoost	Improved accuracy is needed, missing precise labels	Accuracy: 84%
C. Chen et al. [22]	The Fifth Medical Center of the PLA General Hospital	3D-Attention U-Net	Deficiencies in the dataset	Accuracy: 94.43%
Kim. et al. [23]	Seoul St. Mary's Hospital dataset	DenseNet2 01	Inadequate data	Sensitivity: 96.2%
Lu et al. [24]	RIDER	Marine-predator-based 2-D CNN	Inadequate data	Accuracy: 93%
Nasser et al. [25]	Private Lung Dataset	ANN	Necessitate handcrafted features	Accuracy: 96.67%
Agarwal et al. [26]	Private Lung Dataset	AlexNet CNN	inadequate data, deficiencies in the dataset	Accuracy: 96.0%
Mosavi et al. [27]	Luna 16	LeNet, AlexNet, VGG16, ResNet-50, and Inception-V1, with the Adam, RMSprop, and SGD optimizers	The impact of randomness can be removed by modifications to varying optimizers.	Accuracy: 97.42% for AlexNet architecture with the SGD-optimizer
Khehrah et al. [28]	LIDC-IDRI	ANN	Necessitate handcrafted features	Accuracy: 96.25%

B. Dataset Description

The (IQ -OTH/NCCD) LC data has been compiled over three months at specific hospitals in 2019. It consists of CT scans of both people in good health and LC patients with various illness types. Overall, the collection consists of 1190 pictures from 110 CT scans. Three categories: benign, malignant, and normal, are used to categorize these images, 40 of them have been determined to be malignant, 15 to be benign, and 55 to be normal cases [29], the dataset can be accessed and downloaded at [30], Fig. 2. Shows a sample of the CT scan slices.



Figure 2: Sample of CT scan slices.

C. Data Preprocessing

The used dataset contains actual data that has certain quality issues, lack of some values, inconsistencies, and noise. The preparation step of the data has a crucial role to help remove inconsistencies, eliminate duplicates, and normalize the data on hand [31], Fig. 3. Shows the procedures that were performed in the preprocessing phase. The preprocessing steps go as follows: First, Noise reduction is performed to take out any artifacts that aren't related to the original image content which is believed to be a variation in statistics in an estimation created by an occurrence at random. Noise in imagery happens to be a defect that resembles a granular texture over the image, A 2D median filter with a 3x3 dimension is used to eliminate digitization of noise from the CT image. Instead of replacing each pixel's grey level with its average value, the median filter functions by utilizing the median of the grey levels in the near vicinity of the pixels, when the median filter crosses an edge, fresh, erroneous pixel values are not produced. For this reason, the median filter outperforms the mean filter when it comes to maintaining sharp edges[32]. To improve the contrast of images, histogram equalization is utilized by altering intensity image values to produce an output image with a roughly flat histogram by applying a classical histogram equalization method [33][34]. After that, morphology operations are performed to enhance image quality and increase the accuracy of segmentation results before segmentation, This image processing technique can be thought of as processing images while considering the shape[35]. These operations take into account adding a structural component to a source image to produce a comparable-sized output image. Each output image pixel's estimates in such a process take into account the correlation between that pixel and its neighboring pixels. [36]depending on its use, it can take many different forms. Erosion and dilation are the most frequent and fundamental morphological processes, while erosion entails eliminating pixels from item borders, Dilation comprises the inclusion of pixels to object boundaries in an image. Depending on the dimensions and shape of the framework component used during the processing of the image, a specific amount of pixels could be added or even taken away from the image's composition[37]. In these morphological processes, it is possible to determine the state of any individual pixel in the image that is produced through the application of a rule to the evaluated pixel and its neighbors in the original image [38]. In our work Erosion assisted in reducing and marginating the tumor, allowing it to be isolated from surrounding tissues and later processed.

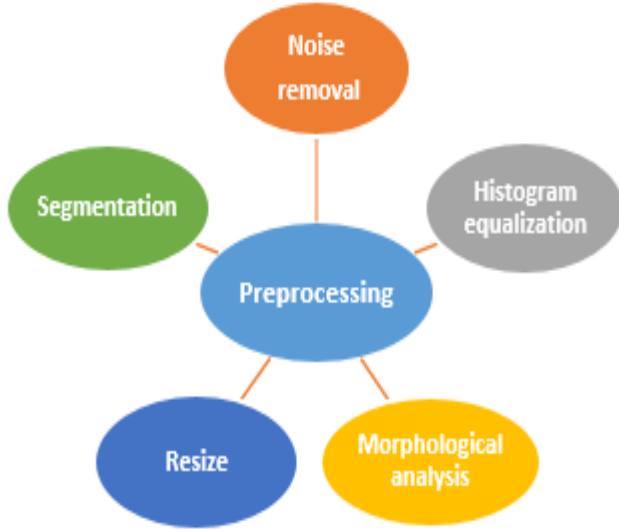


Figure 3. The procedures of the preprocessing phase

To cut down on computation time, the tumor patches in this study are digitally extracted using methods for segmenting before learning[8]. Each grayscale image was then quantized, stored in 24-bit RGB JPEG format at 256 x 256 resolution, and scaled to the dimensions of the 3-channel entry layers in the networks[39]. When a considerable amount of data is utilized for training, DL models perform better, and augmentation approaches can produce a range of images, which can increase the effectiveness of models in applying what they have learned to previously unexplored images. The technique of augmenting the data is applied for generating fresh data to train from an existing training set [40]. It helps increase the size of a dataset without needing to gather additional datasets. A clockwise rotation of 90, 180, 270, and 360 degrees is applied to the segmented images. Every image that has been rotated is then vertically inverted. Eight images will be generated from a single input image in this manner [41].

D. Transfer-Learning (TL)

The established image dataset collection was treated to TL algorithms to set up the testing and training network respectively and assist in the future prediction of new records, specifically VGG 16, VGG 19, and InceptionV3 were used, based on related previous studies these models achieved acceptable performance levels on different datasets [42][43][44] [45]. Over the past two decades, deep learning has provided solutions to a variety of machine learning issues[46]. It does have two important drawbacks, though: the need for large amounts of labeled data and the high expense of training. By reusing learned information from the origin of data while training and applying a target set of data, TL seeks to reduce this reliance and associated costs [47][48]. On the ImageNet dataset, several CNN architectures were trained, and they all produced high-accuracy results. Instead of starting the weights at random, we can classify another dataset using these weights. [49]TL uses four different ways.

Table 2. Training values

Parameter	Value
Learning Rate	0.0001
Epochs	20
Optimizer	SGDM
Learning rate drop factor	0.5
Minimum batch size	10

The first approach entails removing the original fully linked layers which serve as classifiers, freezing the weights across the whole network, using the CNN pre-trained layers to acquire features, and adding a classifier layer like a fully linked layer or an alternate classifier using machine learning, like Support Vector Machine as in the method we used. The second method involves removing the initial fully linked layers, fine-tuning the network weights using a very low learning rate, and adding a fresh classifying layer that is appropriate for the newly formed task. The third method consists of removing the fully linked layers, only those upper layers being adjusted while leaving the bottom layers fixed, the next step is the addition of an entirely novel classifier layer that is appropriate for the task at hand. According to some experts, the bottom layers only record fundamental properties like sides and circular shapes, whereas the upper layers collect additional datasets' particular qualities [49]. In light of this, several authors suggest simply fine-tuning the upper layers [50][51]. The fourth approach is to start training a cutting-edge architecture from the base upwards using just those architectures that are successful in addressing a wide range of datasets.

In our research, the networks are tuned integrating the statistical-gradient-descent (SGD) method with momentum (SGDM), a boosted variant of SGD with the training values indicated in Table 2. Even in the case of dimensions with constant gradients, SGDM aims to enhance speed. [52][53].

IV. TRANSFER-LEARNING ARCHITECTURE

Various architectural types, including VGG16, VGG19, and InceptionV3, are compared and studied with the aforementioned model. These designs were selected for this experiment due to their superior image-processing abilities and because they comprise some of the best and most dependable architectures mentioned in the literature. The features are categorized using a linear SVM with a one-vs-all strategy. Although most deep learning models use the softmax activation function for classification tasks, it has been demonstrated that SVM performs better on several widely used datasets, including MNIST, CIFAR-10, and the facial expression recognition challenge from the 2013 Representation Learning Workshop [54][55], Fig. 5 demonstrates the TL process.

A. VGG16

Simonyan et al. announced the VGG layout in 2014 [56][57]. The distinguishing features of the VGG family include the stacked 3x3 layers of convolution and an aspect of depth that keeps increasing. With maximum pooling, the volume size is reduced [58]. The ideal prominent VGG16 trait is that it prioritized featuring 3x3 convolution layers with a stride 1 and

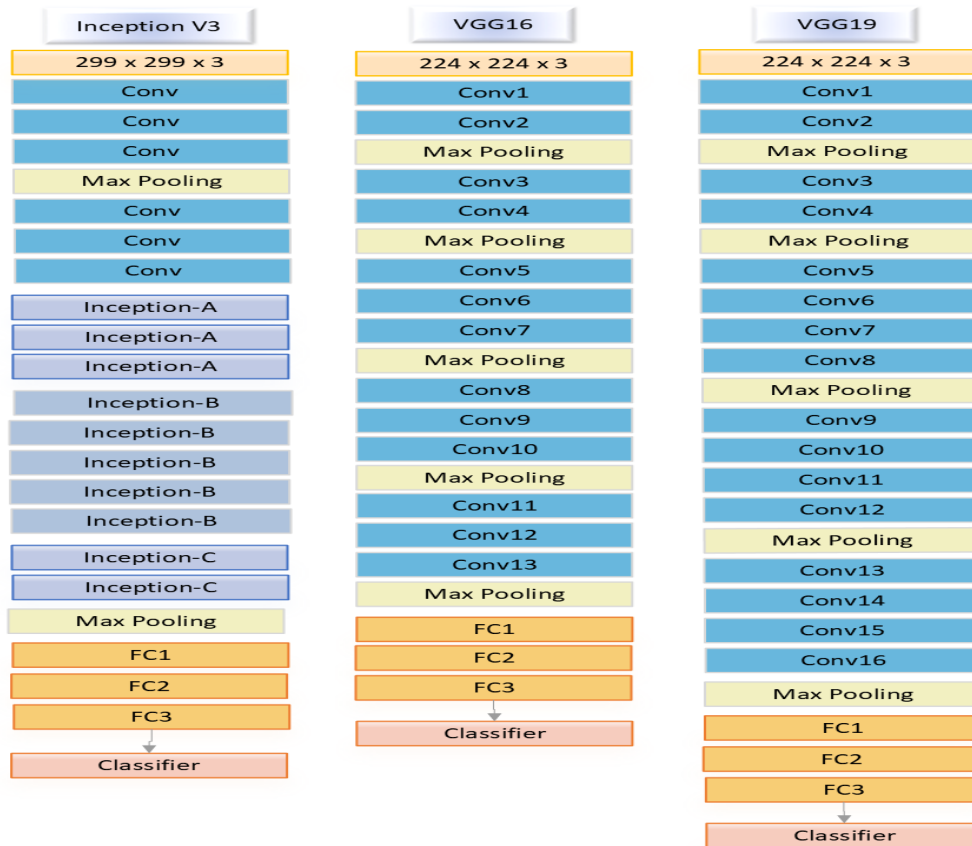


Figure 4. Inception V3, VGG16, VGG19 architecture

2x2 maxpool layers with stride 2, preference over emphasizing containing plenty of hyper-parameters. This arrangement is maintained throughout the system for the convolution and the output is handled by the maxpool layers, three fully linked layers, and a softmax. [59], a demonstration of the basic VGG16 network is shown in Fig. 4. As indicated by the number 16, VGG16 is made up of 16 scaled layers. VGG necessitates a 224x224 RGB image as its input, After receiving the image as input, the VGG convolution network calculates the mean RGB value of the training set image, It uses a 3x3 or 1x1 filter, and the convolution step is fixed[60].

B. VGG19

VGG19 was proposed in early 2014 by Zisserman and Simonyan [56]. It has a softmax layer, five maxpool layers, three fully linked layers, and sixteen convolution layers as shown in Fig. 4. Though the number of layers it supports differs, VGG 19 and VGG 16 are fundamentally equivalent[61]. The image in RGB provided as an input has a constant matrix size of (224, 224, 3)[62]. The RGB mean value of each pixel is removed during preprocessing. To cover the entire image concept, A 1-pixel striding has been applied with kernels of size (3, 3)[63].

When spatial padding is used, the image's spatial resolution is maintained, Two pixels are strided during the (2, 2) max pooling. To incorporate non-linearity into the model and improve classification accuracy while speeding up computation, rectified linear unit, or ReLu is used after this[64], Compared to earlier models like the tanh or sigmoid function, this one performed significantly better[65], followed by Three fully linked layers and it is preceded by a final classification function (Softmax)[5].

C. Inception V3

Szegedy et al. introduced the "Inception" module, which led to the creation of the Inception architecture, as another Google innovation. They released the article "Convolution Deeper" in 2014[66]. Fig.4. demonstrates a simplified representation of InceptionV3 architecture. Compared to VGG, Inception designs are less memory-intensive, meaning they are easier for computers to run. Considering that, it did turn out to function well. [58]. On the ImageNet dataset, InceptionV3 showed an accuracy rate higher than 78.1%[67], The model represents the confluence of numerous concepts created by numerous researchers over time [68].

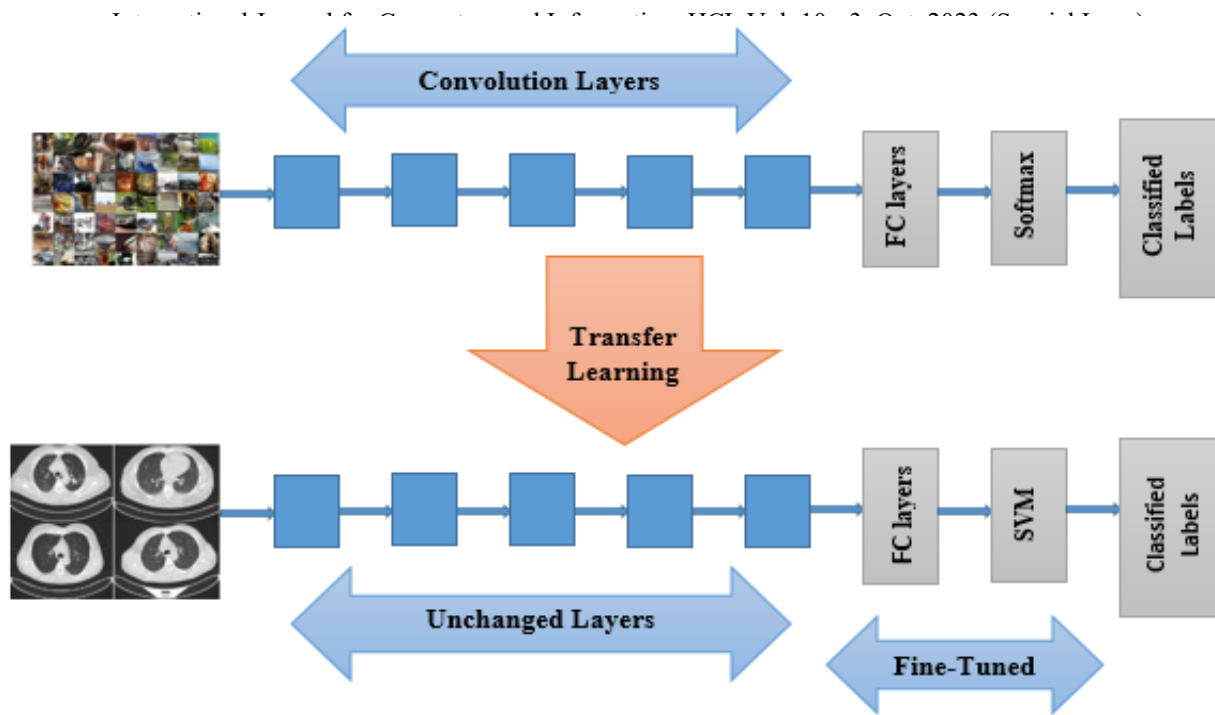


Figure 5. Transfer-Learning settings

InceptionV3 commonly uses one-to-one convolutional kernels to trim the total number of channels for features and expedite training. Additionally, the massive convolution is split up into smaller in-size convolutions, reducing the computational expense and parameter count. In conclusion [69].

V. RESULTS AND DISCUSSION

LC is one of the most fatal and prevalent types of cancer. Depending upon the disease's stage of discovery, this risk may occur. The experiment conducted for the evaluation of the suggested model's functionality on the dataset is summarized in this section. The accuracy, precision, F1- scores, and recall of three DL models (Inception V3, VGG16, and VGG19) using TL are compared in this study after The application of processing of images techniques, which comprises the process of enhancing, segmenting, and extracting features that were done first, then feature selection was done, and finally, images were classified utilizing the stated DL models. Three distinct classes "Benign, Malignant, and Normal" were used to categorize the dataset. The training and testing tasks were then divided into two groups of 80% and 20%. The effectiveness of experimental research was assessed utilizing a confusion-matrix. In the confusion matrix, there are four distinct performance metrics where actual and anticipated records are kept to produce various metrics.

The ratio of positive and negative records that have been successfully discovered is in notion here as "True Positive" and "True Negative", "False Positive", as well as "False Negative" records, are the number of records that correspond to wrongfully predicted positive and negative classifications, correspondingly[70]. The assessment measures for three classes, as stated in Table 2, were put to use to investigate how effective the proposed approach is, The outcomes displayed in Table 3 demonstrate that when using the softmax classifier to diagnose LC, the VGG19 delivers the very best outcomes when it relates to TL, the Experimental results show that the trained model has gained an overall accuracy of 97.1%for VGG19, 96.1%for VGG16, and 95.08%for InceptionV3. While Table 4 shows the accuracy of the model presented after using the SVM classifier, in accordance with the experimental findings, the trained model has improved its overall accuracy by 98% for VGG19, 97.39% for VGG16, and 96.74% for Inception V3, Results from the SVM classifier outperformed those from the Softmax classifier. The evaluations in Table 5 & Fig. 6 compared the outcomes of the proposed model with seven other existing models and show that the analysis results show that it performs more accurately than the other existing models.

Table 2. Performance Evaluation Metrics

Evaluation metrics	Formula	Description
Accuracy	$\frac{\text{No. of truly classified samples}}{\text{Total no. of samples}}$	It describes how effectively the model performs across classes.
Precision	$\frac{\text{True Positive}}{\text{True positive} + \text{False Positive}}$	It is defined as the ratio of relevant outcomes that were predicted to those that occurred, It is referred to as a positive value for prediction, It considers false positives.
Recall	$\frac{\text{True Positive}}{\text{True Positive} + \text{False Negative}}$	It is the ratio of actual to accurately predicted outcomes. It is also known as sensitivity. False negatives are considered.
F-score	$2 * \frac{\text{Precision} * \text{Recall}}{\text{Precision} + \text{Recall}}$	It is the precision and recall's symmetrical mean.

Table 3. LC classification performance measurements using Softmax

Pre-trained Network	Class	Performance measurements per class			
		Accuracy	Recall	Precision	F-score
VGG16	Benign	96.75%	0.93	0.89	0.91
	Malignant	98.05%	0.97	1.0	0.98
	Normal	97.4%	0.97	0.93	0.95
VGG19	Benign	98.07%	0.96	0.90	0.93
	Malignant	97.58%	0.98	0.97	0.98
	Normal	98.55%	0.96	1.0	0.98
INCEPTION V3	Benign	95.08%	0.85	0.92	0.88
	Malignant	98.36%	0.97	1.0	0.99
	Normal	96.72%	1.0	0.86	0.92

Table 4. LC classification performance measurements using SVM

Pre-trained Network	Class	Performance measurements per class			
		Accuracy	Recall	Precision	F-score
VGG16	Benign	97.83%	0.86	0.96	0.91
	Malignant	98.7%	0.99	0.98	0.99
	Normal	98.26%	0.99	0.97	0.98
VGG19	Benign	98.5%	0.92	0.96	0.94
	Malignant	98%	0.99	0.97	0.98
	Normal	99.5%	0.98	1.0	0.99
INCEPTION V3	Benign	97.67%	0.93	0.90	0.92
	Malignant	98.6%	0.98	0.99	0.99
	Normal	97.21%	0.96	0.96	0.96

Table 5. Comparing the suggested model with other existing models utilizing the same dataset

Author	Year	Used method	Accuracy
AL-Huseiny <i>et al</i> [71]	2021	GoogleNet	94.38%
Al-Yasriy <i>et al</i> [72]	2020	AlexNet	93.548%
H. F. Kareem <i>et al</i> [73]	2021	SVM	89.88%
Proposed	2023	VGG16-SVM	97.39%
		VGG19-SVM	98%
		InceptionV3-SVM	96.74%

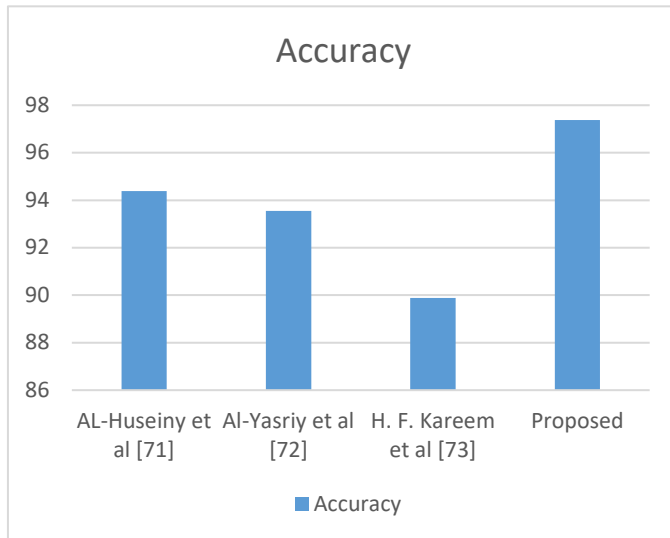


Figure 6. Accuracy comparison representation of the proposed approach and comparable models using the same dataset

CONCLUSION

Our study's goal explains how DL is adapted to automatically detect and classifies cancer in CT scans. This planned study seeks to halt the further progression of LC by detecting nodules early. To accomplish this, this study proposes an effective computer-aided medical diagnostics approach for the rapid identification of this lethal lesion. In this case, chest tomography images were used as the data source for the suggested model. The proposed method surpasses as well as compared to other algorithms utilized on different datasets. F1-score, recall, and precision were among the other performance metrics that were computed. This method can be used to correctly classify medical images, according to these criteria, which support the conclusion reached above. The method being proposed also raises the possibility of growing the usage of pre-trained models as a means of making up for a shortage of resources for computation in academic and medical institutions. To further develop this work in forthcoming studies, the model's satisfactory accuracy can be regularly checked by training it on more and more substantial datasets. Additionally, merging several machine learning models enables comparison, several optimizers can be used to reduce the randomness effect and increase accuracy.

REFERENCES

[1] M. E. Tschuchnig and M. Gademayr, "Anomaly detection in medical imaging-a mini review," in *Data Science-Analytics and Applications: Proceedings of the 4th International Data Science Conference-iDSC2021*, 2022, pp. 33–38.

[2] N. J. Wald, M. Idle, J. Boreham, and A. Bailey, "Inhaling and lung cancer: an anomaly explained.," *Br Med J (Clin Res Ed)*, vol. 287, no. 6401, pp. 1273–1275, 1983.

[3] J. Huang *et al.*, "Distribution, risk factors, and temporal trends for

lung cancer incidence and mortality: a global analysis," *Chest*, vol. 161, no. 4, pp. 1101–1111, 2022.

[4] M. Kuschner, "The J. Burns Amberson lecture: the causes of lung cancer," *Am. Rev. Respir. Dis.*, vol. 98, no. 4, pp. 573–590, 1968.

[5] A. Mohite, "Application of transfer learning technique for detection and classification of lung cancer using CT images," *Int J Sci Res Manag*, vol. 9, no. 11, pp. 621–634, 2021.

[6] W. Mapanga *et al.*, "Consensus study on the health system and patient-related barriers for lung cancer management in South Africa," *PLoS One*, vol. 16, no. 2, p. e0246716, 2021.

[7] A. Motohiro, H. Ueda, H. Komatsu, N. Yanai, T. Mori, and N. C. H. S. G. for L. Cancer, "Prognosis of non-surgically treated, clinical stage I lung cancer patients in Japan," *Lung cancer*, vol. 36, no. 1, pp. 65–69, 2002.

[8] J. Kuruvilla, D. Sukumaran, A. Sankar, and S. P. Joy, "A review on image processing and image segmentation," in *2016 international conference on data mining and advanced computing (SAPIENCE)*, 2016, pp. 198–203.

[9] G. Zhang *et al.*, "Automatic nodule detection for lung cancer in CT images: A review," *Comput. Biol. Med.*, vol. 103, pp. 287–300, 2018.

[10] A. A. Meldo and L. V. Utkin, "A new approach to differential lung diagnosis with ct scans based on the siamese neural network," in *Journal of Physics: Conference Series*, 2019, vol. 1236, no. 1, p. 12058.

[11] A. L. Chong, R. V. Chandra, K. C. Chuah, E. L. Roberts, and S. L. Stuckey, "Proton density MRI increases detection of cervical spinal cord multiple sclerosis lesions compared with T2-weighted fast spin-echo," *Am. J. Neuroradiol.*, vol. 37, no. 1, pp. 180–184, 2016.

[12] S. Al-Zeibak and N. H. Saunders, "A feasibility study of in vivo electromagnetic imaging," *Phys. Med. Biol.*, vol. 38, no. 1, p. 151, 1993.

[13] R. Merwa, K. Hollaus, P. Brunner, and H. Scharfetter, "Solution of the inverse problem of magnetic induction tomography (MIT)," *Physiol. Meas.*, vol. 26, no. 2, p. S241, 2005.

[14] F. Zhuang *et al.*, "A comprehensive survey on transfer learning," *Proc. IEEE*, vol. 109, no. 1, pp. 43–76, 2020.

[15] T. I. A. Mohamed, "Optimized deep learning model for early detection and classification of lung cancer on CT images." 2022.

[16] B. Akay, D. Karaboga, and R. Akay, "A comprehensive survey on optimizing deep learning models by metaheuristics," *Artif. Intell. Rev.*, pp. 1–66, 2022.

[17] G. Hemanth, M. Janardhan, and L. Sujihelen, "Design and implementing brain tumor detection using machine learning approach," in *2019 3rd international conference on trends in electronics and informatics (ICOEI)*, 2019, pp. 1289–1294.

[18] M. Nazir, S. Shakil, and K. Khurshid, "Role of deep learning in brain tumor detection and classification (2015 to 2020): A review," *Comput. Med. Imaging Graph.*, vol. 91, p. 101940, 2021.

[19] S. Wang, L. Dong, X. Wang, and X. Wang, "Classification of pathological types of lung cancer from CT images by deep residual neural networks with transfer learning strategy," *Open Med.*, vol. 15, no. 1, pp. 190–197, 2020.

[20] S. Zheng *et al.*, "Interpretative computer-aided lung cancer diagnosis: From radiology analysis to malignancy evaluation," *Comput. Methods Programs Biomed.*, vol. 210, p. 106363, 2021.

[21] S. Bhatia, Y. Sinha, and L. Goel, "Lung cancer detection: a deep learning approach," in *Soft Computing for Problem Solving: SocProS 2017, Volume 2*, 2019, pp. 699–705.

[22] C. Chen *et al.*, "An effective deep neural network for lung lesions segmentation from COVID-19 CT images," *IEEE Trans. Ind. Informatics*, vol. 17, no. 9, pp. 6528–6538, 2021.

[23] H. M. Kim, T. Ko, I. Y. Choi, and J.-P. Myong, "Asbestosis diagnosis algorithm combining the lung segmentation method and deep learning model in computed tomography image," *Int. J. Med. Inform.*, vol. 158, p. 104667, 2022.

[24] X. Lu, Y. A. Nanehkaran, and M. Karimi Fard, "A method for optimal detection of lung cancer based on deep learning optimized by marine predators algorithm," *Comput. Intell. Neurosci.*, vol. 2021, 2021.

[25] I. M. Nasser and S. S. Abu-Naser, "Lung cancer detection using artificial neural network," *Int. J. Eng. Inf. Syst.*, vol. 3, no. 3, pp. 17–23, 2019.

- [26] A. Agarwal, K. Patni, and D. Rajeswari, "Lung cancer detection and classification based on alexnet CNN," in *2021 6th International Conference on Communication and Electronics Systems (ICCES)*, 2021, pp. 1390–1397.
- [27] I. Naseer, S. Akram, T. Masood, A. Jaffar, M. A. Khan, and A. Mosavi, "Performance analysis of state-of-the-art CNN architectures for luna16," *Sensors*, vol. 22, no. 12, p. 4426, 2022.
- [28] N. Khehrah, M. S. Farid, S. Bilal, and M. H. Khan, "Lung nodule detection in CT images using statistical and shape-based features," *J. Imaging*, vol. 6, no. 2, p. 6, 2020.
- [29] H. Alyasriy and A. H. Muayed, "The IQ-OTHNCCD lung cancer dataset," *Mendeley Data*, vol. 1, no. 1, pp. 1–13, 2020.
- [30] "No Title."
- [31] S. Abunajm, N. Elsayed, Z. ElSayed, and M. Ozer, "Deep Learning Approach for Early Stage Lung Cancer Detection," *arXiv Prepr. arXiv2302.02456*, 2023.
- [32] A. Shah *et al.*, "Comparative analysis of median filter and its variants for removal of impulse noise from gray scale images," *J. King Saud Univ. Inf. Sci.*, vol. 34, no. 3, pp. 505–519, 2022.
- [33] S. Patel and M. Goswami, "Comparative analysis of Histogram Equalization techniques," in *2014 International Conference on Contemporary Computing and Informatics (IC3I)*, 2014, pp. 167–168.
- [34] C. R. Nithyananda and A. C. Ramachandra, "Review on histogram equalization based image enhancement techniques," in *2016 International Conference on Electrical, Electronics, and Optimization Techniques (ICEEOT)*, 2016, pp. 2512–2517.
- [35] M. Goyal, "Morphological image processing," *IJCST*, vol. 2, no. 4, p. 59, 2011.
- [36] S. Uzelaltinbulat and B. Ugur, "Lung tumor segmentation algorithm," *Procedia Comput. Sci.*, vol. 120, pp. 140–147, 2017.
- [37] A. S. Ahmed, A. E. Keshk, O. M Abo-Seida, and M. Sakr, "Tumor detection and classification in breast mammography based on fine-tuned convolutional neural networks," *IJCI. Int. J. Comput. Inf.*, vol. 9, no. 1, pp. 74–84, 2022.
- [38] R. C. Gonzalez, *Digital image processing*. Pearson education india, 2009.
- [39] S. Perumal and T. Velmurugan, "Preprocessing by contrast enhancement techniques for medical images," *Int. J. Pure Appl. Math.*, vol. 118, no. 18, pp. 3681–3688, 2018.
- [40] K. Maharana, S. Mondal, and B. Nemade, "A review: Data preprocessing and data augmentation techniques," *Glob. Transitions Proc.*, 2022.
- [41] M. Xu, S. Yoon, A. Fuentes, and D. S. Park, "A comprehensive survey of image augmentation techniques for deep learning," *Pattern Recognit.*, p. 109347, 2023.
- [42] R. Jain, P. Nagrath, G. Kataria, V. S. Kaushik, and D. J. Hemanth, "Pneumonia detection in chest X-ray images using convolutional neural networks and transfer learning," *Measurement*, vol. 165, p. 108046, 2020.
- [43] M. Effati and G. Nejat, "A Performance Study of CNN Architectures for the Autonomous Detection of COVID-19 Symptoms Using Cough and Breathing," *Computers*, vol. 12, no. 2, p. 44, 2023.
- [44] G. Labhane, R. Pansare, S. Maheshwari, R. Tiwari, and A. Shukla, "Detection of pediatric pneumonia from chest X-ray images using CNN and transfer learning," in *2020 3rd international conference on emerging technologies in computer engineering: machine learning and internet of things (ICETCE)*, 2020, pp. 85–92.
- [45] M. A. R. Ratul, M. H. Mozaffari, W.-S. Lee, and E. Parimbelli, "Skin lesions classification using deep learning based on dilated convolution," *BioRxiv*, p. 860700, 2019.
- [46] E. Hassan, M. Y. Shams, N. A. Hikal, and S. Elmougy, "COVID-19 diagnosis-based deep learning approaches for COVIDx dataset: A preliminary survey," *Artif. Intell. Dis. Diagnosis Progn. Smart Healthc.*, vol. 107, 2023.
- [47] M. Iman, H. R. Arabnia, and K. Rasheed, "A review of deep transfer learning and recent advancements," *Technologies*, vol. 11, no. 2, p. 40, 2023.
- [48] J. Deng, W. Dong, R. Socher, L.-J. Li, K. Li, and L. Fei-Fei, "Imagenet: A large-scale hierarchical image database," in *2009 IEEE conference on computer vision and pattern recognition*, 2009, pp. 248–255.
- [49] I. Kandel and M. Castelli, "Transfer learning with convolutional neural networks for diabetic retinopathy image classification. A review," *Appl. Sci.*, vol. 10, no. 6, p. 2021, 2020.
- [50] H.-C. Shin *et al.*, "Deep convolutional neural networks for computer-aided detection: CNN architectures, dataset characteristics and transfer learning," *IEEE Trans. Med. Imaging*, vol. 35, no. 5, pp. 1285–1298, 2016.
- [51] S. Kornblith, J. Shlens, and Q. V Le, "Do better imagenet models transfer better?," in *Proceedings of the IEEE/CVF conference on computer vision and pattern recognition*, 2019, pp. 2661–2671.
- [52] A. Saber, M. Sakr, O. M. Abo-Seida, A. Keshk, and H. Chen, "A novel deep-learning model for automatic detection and classification of breast cancer using the transfer-learning technique," *IEEE Access*, vol. 9, pp. 71194–71209, 2021.
- [53] E. Hassan, M. Y. Shams, N. A. Hikal, and S. Elmougy, "The effect of choosing optimizer algorithms to improve computer vision tasks: a comparative study," *Multimed. Tools Appl.*, vol. 82, no. 11, pp. 16591–16633, 2023.
- [54] Y. Tang, "Deep learning using linear support vector machines," *arXiv Prepr. arXiv1306.0239*, 2013.
- [55] W. Zhang, B. Pogorelsky, M. Loveland, and T. Wolf, "Classification of COVID-19 X-ray images using a combination of deep and handcrafted features," *arXiv Prepr. arXiv2101.07866*, 2021.
- [56] K. Simonyan and A. Zisserman, "Very deep convolutional networks for large-scale image recognition," *arXiv Prepr. arXiv1409.1556*, 2014.
- [57] S. B. Stoecklin *et al.*, "First cases of coronavirus disease 2019 (COVID-19) in France: surveillance, investigations and control measures, January 2020," *Eurosurveillance*, vol. 25, no. 6, p. 2000094, 2020.
- [58] S. Guefrechi, M. Ben Jabra, A. Ammar, A. Koubaa, and H. Hamam, "Deep learning based detection of COVID-19 from chest X-ray images," *Multimed. Tools Appl.*, vol. 80, pp. 31803–31820, 2021.
- [59] S. Mascarenhas and M. Agarwal, "A comparison between VGG16, VGG19 and ResNet50 architecture frameworks for Image Classification," in *2021 International Conference on Disruptive Technologies for Multi-Disciplinary Research and Applications (CENTCON)*, 2021, vol. 1, pp. 96–99.
- [60] D. Theckedath and R. R. Sedamkar, "Detecting affect states using VGG16, ResNet50 and SE-ResNet50 networks," *SN Comput. Sci.*, vol. 1, pp. 1–7, 2020.
- [61] M. Simon, E. Rodner, and J. Denzler, "Imagenet pre-trained models with batch normalization," *arXiv Prepr. arXiv1612.01452*, 2016.
- [62] A. V. Ikechukwu, S. Murali, R. Deepu, and R. C. Shivamurthy, "ResNet-50 vs VGG-19 vs training from scratch: A comparative analysis of the segmentation and classification of Pneumonia from chest X-ray images," *Glob. Transitions Proc.*, vol. 2, no. 2, pp. 375–381, 2021.
- [63] T. Carvalho, E. R. S. De Rezende, M. T. P. Alves, F. K. C. Balieiro, and R. B. Sovat, "Exposing computer generated images by eye's region classification via transfer learning of VGG19 CNN," in *2017 16th IEEE international conference on machine learning and applications (ICMLA)*, 2017, pp. 866–870.
- [64] M. Shaha and M. Pawar, "Transfer learning for image classification," in *2018 second international conference on electronics, communication and aerospace technology (ICECA)*, 2018, pp. 656–660.
- [65] J.-L. Cui, S. Qiu, M. Jiang, Z.-L. Pei, and Y.-N. Lu, "Text classification based on ReLU activation function of SAE algorithm," in *Advances in Neural Networks-ISNN 2017: 14th International Symposium, ISNN 2017, Sapporo, Hakodate, and Muroran, Hokkaido, Japan, June 21–26, 2017, Proceedings, Part I 14*, 2017, pp. 44–50.
- [66] K. He, X. Zhang, S. Ren, and J. Sun, "Deep residual learning for image recognition," in *Proceedings of the IEEE conference on computer vision and pattern recognition*, 2016, pp. 770–778.
- [67] A. Krizhevsky, I. Sutskever, and G. E. Hinton, "Imagenet classification with deep convolutional neural networks," *Commun. ACM*, vol. 60, no. 6, pp. 84–90, 2017.
- [68] O. Russakovsky *et al.*, "Imagenet large scale visual recognition challenge," *Int. J. Comput. Vis.*, vol. 115, pp. 211–252, 2015.
- [69] C. Lin, L. Li, W. Luo, K. C. P. Wang, and J. Guo, "Transfer learning

- based traffic sign recognition using inception-v3 model,” *Period. Polytech. Transp. Eng.*, vol. 47, no. 3, pp. 242–250, 2019.
- [70] Z. Wu *et al.*, “Deep learning for classification of pediatric otitis media,” *Laryngoscope*, vol. 131, no. 7, pp. E2344–E2351, 2021.
- [71] M. S. AL-Huseiny and A. S. Sajit, “Transfer learning with GoogLeNet for detection of lung cancer,” *Indones. J. Electr. Eng. Comput. Sci.*, vol. 22, no. 2, pp. 1078–1086, 2021.
- [72] H. F. Al-Yasriy, M. S. AL-Husieny, F. Y. Mohsen, E. A. Khalil, and Z. S. Hassan, “Diagnosis of lung cancer based on CT scans using CNN,” in *IOP Conference Series: Materials Science and Engineering*, 2020, vol. 928, no. 2, p. 22035.
- [73] H. F. Kareem, M. S. AL-Husieny, F. Y. Mohsen, E. A. Khalil, and Z. S. Hassan, “Evaluation of SVM performance in the detection of lung cancer in marked CT scan dataset,” *Indones. J. Electr. Eng. Comput. Sci.*, vol. 21, no. 3, p. 1731, 2021.